

# Lattice QCD constraints on the critical point from an improved precision equation of state

Jana N. Guenther<sup>1,\*</sup>, Szabolcs Borsanyi<sup>1</sup>, Zoltán Fodor<sup>2,3,1,4,5</sup>, Paolo Parotto<sup>6</sup>, Attila Pásztor<sup>4</sup>, Claudia Ratti<sup>7</sup>, Volodymyr Vovchenko<sup>7</sup>, and Chik Him Wong<sup>1</sup>

<sup>1</sup>University of Wuppertal, Department of Physics, Wuppertal D-42119, Germany

<sup>2</sup>Pennsylvania State University, Department of Physics, State College, PA 16801, USA

<sup>3</sup>Pennsylvania State University, Institute for Computational and Data Sciences, State College, PA 16801, USA

<sup>4</sup>Institute for Theoretical Physics, ELTE Eötvös Loránd University, Pázmány P. sétány 1/A, H-1117 Budapest, Hungary

<sup>5</sup>Jülich Supercomputing Centre, Forschungszentrum Jülich, D-52425 Jülich, Germany

<sup>6</sup>Dipartimento di Fisica, Università di Torino and INFN Torino, Via P. Giuria 1, I-10125 Torino, Italy

<sup>7</sup>Department of Physics, University of Houston, Houston, TX 77204, USA

**Abstract.** A recent proposal (Ref. [1]) suggested searching for the QCD critical point by studying contours of constant entropy density on the phase diagram. In our recent work Ref. [2], we refine and extend this method. Our results exclude, at the  $2\sigma$  confidence level, the existence of a critical point at baryon chemical potentials below  $\mu_B \approx 450$  MeV along the transition line.

## 1 Introduction

The study of the QCD phase diagram remains a central goal of both theory and experiment. Lattice QCD calculations have firmly established that, at vanishing baryon chemical potential, the transition is a smooth crossover occurring at temperatures of about 155–160 MeV. At finite chemical potential, many effective models and functional methods predict that the crossover turns into a first-order transition, ending in a critical point. Locating or excluding such a point is therefore one of the key challenges in the field.

Recently, a novel method was proposed in Ref. [1] to constrain the critical point. The approach is based on studying contours of constant entropy density: if such contours overlap on the phase diagram, this signals the onset of a first-order regime, and their intersection can be used to locate the critical endpoint. The analysis in Ref. [1] already demonstrated the potential of this idea using existing lattice data, but was limited by statistical precision and by the use of simplified conditions.

In Ref. [2], we extended and refined this method by combining a new high-precision, continuum-extrapolated equation of state at  $\mu_B = 0$  with lattice simulations at imaginary chemical potential under conditions of strangeness neutrality and including higher orders in the extrapolation.

---

\*e-mail: [jguenther@uni-wuppertal.de](mailto:jguenther@uni-wuppertal.de)

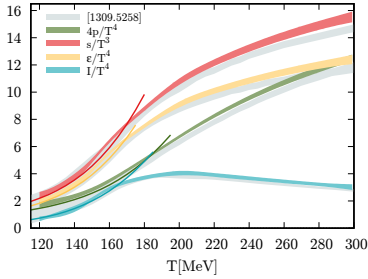


**Figure 1.** Pressure (green), entropy (red), energy density (yellow) and trace anomaly (cyan) as functions of the temperature. The gray bands show our previous results from Ref. [3], while the curves at low temperature are the HRG model results. The deviations between the two sets of data at high temperature are due to the inclusion of the charm quark in our new results, as opposed to the 2+1 flavor result from Ref. [3].

## 2 Improved precision equation of state at $\mu_B = 0$

A central ingredient of our analysis is a new determination of the QCD equation of state (EoS) at vanishing baryon chemical potential. We employ the 4stout staggered fermion action with  $N_f = 2 + 1 + 1$  flavors at physical quark masses, i.e. including the dynamical effects of the charm quark. This extends our previous 2 + 1-flavor results [3] by providing both improved precision and a broader range in temperature.

The pressure is obtained using the *integral method* [4], which reconstructs it from the trace anomaly  $I(T)$ :  $\frac{p(T)}{T^4} = \frac{p(T_0)}{T_0^4} + \int_{T_0}^T \frac{dT'}{T'} \frac{I(T')}{T'^4}$ , with the reference temperature set to  $T_0 = 185$  MeV, which minimizes uncertainties in the transition region.

The trace anomaly itself is defined as  $\frac{I(T)}{T^4} = -TN_\tau^4 \frac{dB}{dT} \left( \langle -s_G \rangle + \sum_f \frac{dm_f}{dB} \langle \bar{\psi}_f \psi_f \rangle \right)$ , where  $\langle -s_G \rangle$  is the gauge action density and  $\langle \bar{\psi}_f \psi_f \rangle$  are the chiral condensates. Both quantities require additive renormalization, which is carried out by subtracting the corresponding vacuum expectation values at zero temperature. For the continuum extrapolation, we use lattices with temporal extents  $N_\tau = 8, 10, 12, 16$ . The finite-spacing data are extrapolated linearly in  $1/N_\tau^2$ , combined with a spline interpolation in temperature. Systematic effects are controlled by repeating the analysis with multiple scale-setting procedures, polynomial orders, and spline parametrizations.

From the pressure and the trace anomaly, all other thermodynamic quantities follow directly. Our results for  $p/T^4$ ,  $s/T^3$ ,  $\epsilon/T^4$ , and  $I/T^4$  are shown in Fig. 1. Compared to our previous work, the new results exhibit substantially reduced uncertainties, especially in the transition region. At high temperatures  $T \gtrsim 250$  MeV, the effect of the charm quark becomes visible, leading to a deviation from the earlier 2 + 1-flavor EoS. At lower temperatures, our results smoothly match the hadron resonance gas model predictions.

In summary, we have established a high-precision determination of the QCD equation of state at  $\mu_B = 0$  in the range  $120 \lesssim T \lesssim 300$  MeV. This serves as the foundation for the construction of entropy contours at imaginary chemical potential, which in turn are used to constrain the location of the QCD critical point.

## 3 Contours of constant entropy for $\mu_B > 0$

With the zero-density equation of state determined at high precision, we can proceed to investigate the QCD phase diagram at finite baryon chemical potential. Since direct lattice simulations at real  $\mu_B$  are obstructed by the sign problem, we rely on analytic continuation from simulations performed at imaginary  $\mu_B$ . The method we employ is based on the study of contours of constant entropy density, an idea first proposed in Ref. [1] and extended in our recent work [2]. The central observation is that the entropy density is a monotonic and continuous function of the temperature in the absence of a first-order transition. If, at some finite chemical potential, the entropy becomes multi-valued, this signals the appearance of a

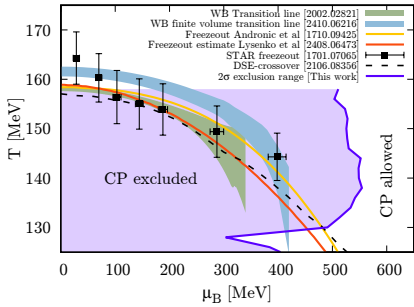


**Figure 2.** The QCD phase diagram with the  $2\sigma$  exclusion range. We also show the chiral transition line from the continuum extrapolated lattice simulations in a large volume [5], as well as a recent result in a smaller system without continuum extrapolation [6] and a prediction based on Dyson-Schwinger equations [7]. Besides the STAR result for chemical freeze-out parameters [8] and its parametrization [9], we add a lower bound estimate within the HRG framework [10].

spinodal region and the onset of a first-order phase transition. The point where monotonicity breaks down corresponds to the critical endpoint. Thus, by following entropy contours from  $\mu_B = 0$  into the  $(T, \mu_B)$ -plane, one can identify whether and where they intersect, providing constraints on the location of the critical point.

**Construction of entropy contours:** At finite  $\mu_B$ , the entropy can be obtained by integrating the derivative of the baryon density:  $s(T, \mu_B) = s(T, 0) + \int_0^{\mu_B} d\mu'_B \frac{\partial n_B(T, \mu'_B)}{\partial T}$ , where  $n_B$  is the baryon number density. To evaluate this expression, we perform lattice simulations at imaginary baryon chemical potential, on lattices with temporal extent  $N_\tau = 10, 12, 16$ . This allows us to compute  $n_B(T, \mu_B)$  and its derivative with respect to  $T$ . A combined fit is then carried out in temperature, chemical potential, and lattice spacing. From this, we construct the entropy density at imaginary chemical potentials and determine the corresponding contours of constant entropy. Each contour is defined by the condition that it crosses the  $\mu_B = 0$  axis at a given reference temperature  $T_0$ . For each value of  $T_0$ , we thus obtain a trajectory  $T_s(\mu_B, T_0)$  representing the temperature at which the entropy density equals its  $\mu_B = 0$  value.

**Analytic continuation:** To continue the entropy contours to real chemical potential, we fit the imaginary- $\mu_B$  results using a rational ansatz,  $T_s(\mu_B^2, T_0) = \frac{T_0 + a\mu_B^2}{1 + b\mu_B^2}$ , where  $a$  and  $b$  are fit parameters. This functional form accommodates the nearly linear dependence observed at imaginary  $\mu_B^2 < 0$ , while allowing for deviations at larger values.

**Identifying the onset of a first-order regime:** To detect the breakdown of monotonicity, we study the slope of  $T_s(\mu_B^2, T_0)$  with respect to  $T_0$  at fixed  $\mu_B$ . In the absence of a first-order transition,  $\left(\frac{\partial T_s}{\partial T_0}\right)_{\mu_B} > 0$ . At the critical point this derivative vanishes, while in the first-order region it becomes negative. Thus, evaluating  $(\partial T_s / \partial T_0)_{\mu_B}$  provides a diagnostic for the presence of a critical endpoint. At larger chemical potentials, the data are consistent with a vanishing or negative derivative within errors.

**Statistical and systematic treatment:** A crucial step in our analysis is the careful treatment of uncertainties. In total, this yields 192 separate analyses, which are described in detail in Ref. [2]. The final outcome is a probability map on the  $(T, \mu_B)$  plane for the entropy contours to exhibit a non-monotonic slope. From this, we determine the minimal  $\mu_B$  at which criticality cannot be excluded at a given confidence level.

**Constraints on the critical point** Our main result is summarized in Fig. 2. We find that, at the  $2\sigma$  confidence level, the existence of a critical point can be excluded below  $\mu_B^{2\sigma} \approx 450$  MeV. This constitutes the first reliable lower bound on the critical chemical potential from continuum-extrapolated lattice QCD. To connect with phenomenology, we overlay our exclusion region with estimates of the chemical freeze-out curve from heavy-ion collisions [8–10] and with predictions of the crossover line from functional methods [7]. Our conservative choice is to compare with the lower bound on freeze-out temperatures

given in Ref. [10]. In this way, we conclude that the experimentally relevant region up to  $\mu_B \approx 450$  MeV is unlikely to host a critical point.

**Acknowledgments.** This work is supported by the MKW NRW under the funding code NW21-024-A. Further funding was received from the DFG under the Project No. 496127839. This work was also supported by the Hungarian National Research, Development and Innovation Office, NKFIH Grant No. KKP126769. This work was also supported by the NKFIH excellence grant TKP2021\_NKTA\_64. This work is also supported by the Hungarian National Research, Development and Innovation Office under Project No. FK 147164. This material is also based upon work supported by the National Science Foundation under grants No. PHY-2514763, PHY-2208724, and PHY-2116686, and within the framework of the MUSES collaboration, under grant number No. OAC- 2103680. This material is also based upon work supported by the U.S. Department of Energy, Office of Science, Office of Nuclear Physics, under Award Numbers DE-SC0022023 and DE-SC0025025, as well as by the National Aeronautics and Space Agency (NASA) under Award Number 80NSSC24K0767. The authors gratefully acknowledge the Gauss Centre for Supercomputing e.V. ([www.gauss-centre.eu](http://www.gauss-centre.eu)) for funding this project by providing computing time on the GCS Supercomputer HAWK at HLRS, Stuttgart. An award of computer time was provided by the INCITE program. This research used resources of the Argonne Leadership Computing Facility, which is a DOE Office of Science User Facility supported under Contract DE-AC02-06CH11357.

## References

- [1] H. Shah, M. Hippert, J. Noronha, C. Ratti, V. Vovchenko, Locating the QCD critical point from first principles through contours of constant entropy density (2024), **2410**.16206.
- [2] S. Borsanyi, Z. Fodor, J.N. Guenther, P. Parotto, A. Pasztor, C. Ratti, V. Vovchenko, C.H. Wong, Lattice QCD constraints on the critical point from an improved precision equation of state (2025), **2502**.10267.
- [3] S. Borsanyi, Z. Fodor, C. Hoelbling, S.D. Katz, S. Krieg, K.K. Szabo, Full result for the QCD equation of state with 2+1 flavors, *Phys. Lett.* **B730**, 99 (2014), **1309**.5258. [10.1016/j.physletb.2014.01.007](https://arxiv.org/abs/10.1016/j.physletb.2014.01.007)
- [4] J. Engels, J. Fingberg, F. Karsch, D. Miller, M. Weber, Nonperturbative thermodynamics of SU(N) gauge theories, *Phys. Lett. B* **252**, 625 (1990). [10.1016/0370-2693\(90\)90496-S](https://arxiv.org/abs/10.1016/0370-2693(90)90496-S)
- [5] S. Borsanyi, Z. Fodor, J.N. Guenther, R. Kara, S.D. Katz, P. Parotto, A. Pasztor, C. Ratti, K.K. Szabo, QCD Crossover at Finite Chemical Potential from Lattice Simulations, *Phys. Rev. Lett.* **125**, 052001 (2020), **2002**.02821. [10.1103/PhysRevLett.125.052001](https://arxiv.org/abs/10.1103/PhysRevLett.125.052001)
- [6] S. Borsanyi, Z. Fodor, J.N. Guenther, P. Parotto, A. Pasztor, L. Pirelli, K.K. Szabo, C.H. Wong, QCD deconfinement transition line up to  $\mu_B=400$  MeV from finite volume lattice simulations, *Phys. Rev. D* **110**, 114507 (2024), **2410**.06216. [10.1103/PhysRevD.110.114507](https://arxiv.org/abs/10.1103/PhysRevD.110.114507)
- [7] P.J. Gunkel, C.S. Fischer, Locating the critical endpoint of QCD: Mesonic back-coupling effects, *Phys. Rev. D* **104**, 054022 (2021), **2106**.08356. [10.1103/PhysRevD.104.054022](https://arxiv.org/abs/10.1103/PhysRevD.104.054022)
- [8] L. Adamczyk et al. (STAR), Bulk Properties of the Medium Produced in Relativistic Heavy-Ion Collisions from the Beam Energy Scan Program, *Phys. Rev. C* **96**, 044904 (2017), **1701**.07065. [10.1103/PhysRevC.96.044904](https://arxiv.org/abs/10.1103/PhysRevC.96.044904)
- [9] A. Andronic, P. Braun-Munzinger, K. Redlich, J. Stachel, Decoding the phase structure of QCD via particle production at high energy, *Nature* **561**, 321 (2018), **1710**.09425. [10.1038/s41586-018-0491-6](https://arxiv.org/abs/10.1038/s41586-018-0491-6)
- [10] A. Lysenko, M.I. Gorenstein, R. Poberezhniuk, V. Vovchenko, Chemical freeze-out curve in heavy-ion collisions and the QCD critical point, *Phys. Rev. C* **111**, 054903 (2025), **2408**.06473. [10.1103/PhysRevC.111.054903](https://arxiv.org/abs/10.1103/PhysRevC.111.054903)